J. Phys. B: At. Mol. Opt. Phys. **45** (2012) 145101 (5pp) doi:10.1088/0953-4075/45/14/145101

The $D^1\Pi_u$ state of HD and the mass scaling relation of its predissociation widths

G D Dickenson and W Ubachs

Institute for Lasers, Life and Biophotonics Amsterdam, VU University, de Boelelaan 1081, 1081HV, Amsterdam, The Netherlands

E-mail: w.m.g.ubachs@vu.nl

Received 26 April 2012, in final form 24 May 2012
Published 2 July 2012
Online at stacks.iop.org/JPhysB/45/145101

Abstract
Absorption spectra of HD have been recorded in the wavelength range of 75–90 nm at 100 K using the vacuum ultraviolet Fourier transform spectrometer at the Synchrotron SOLEIL. The present wavelength resolution represents an order of magnitude improvement over that of previous studies. We present a detailed study of the $D^1\Pi_u$–$X^1\Sigma_g^+$ system observed up to $v' = 18$. The Q-branch transition probing levels of Π^- symmetry are observed as narrow resonances limited by the Doppler width at 100 K. Line positions for these transitions are determined to an estimated absolute accuracy of 0.06 cm^{-1}. Predissociation line widths of Π^+ levels are extracted from the absorption spectra. A comparison with the recent results on a study of the $D^1\Pi_u$ state in H_2 and D_2 reveals that the predissociation widths scale as $\mu^{-2}J(J+1)$, with μ being the reduced mass of the molecule and J the rotational angular momentum quantum number, as expected from an interaction with the $B'^1\Sigma_u^+$ continuum causing the predissociation.

(Some figures may appear in colour only in the online journal)

1. Introduction

Since the early years of quantum mechanics the hydrogen molecule has been studied and has provided theorist with an ideal testing ground for calculations. The stable isotopic variants of H_2, namely D_2 and HD, allow for testing mass scaling effects. The $D^1\Pi_u$ state was found to undergo predissociation above the third vibrational level (the fourth vibrational level for D_2 and HD) which can be accurately described by Fano's theory of a single bound state interacting with a continuum (Fano 1961).

The $D^1\Pi_u$ state of HD has received considerably less interest compared to the other two stable isotopic variants. On the experimental side Takezawa and Tanaka (1972) determined $Q(1)$ transitions for the lowest three vibrations accurate to within a few cm^{-1}. Monfils (1965) measured level energies for both Π^+ and Π^- parity components up to $v' = 8$ with accuracies of $\sim$5 cm^{-1}. A profile analysis of the predissociated line shapes was conducted by Dehmer and Chupka for $v' = 7$ and 9 as well as a separate study focusing on the line positions for the $R(0)$, $R(1)$ and $Q(1)$ transitions from $v' = 7$–16 (Dehmer and Chupka 1980, 1983) with accuracies of $\sim$4 cm^{-1}. Theoretically, Kołos and Rychlewski (1976) have calculated the vibrational levels up to the $n = 3$ dissociation limit for the $D^1\Pi_u$ state , while Abgrall and Roueff (2006) calculated term values for the lowest three vibrations ($v' = 0$–2) in a study focusing mainly on the Lyman and Werner bands of HD.

This work on HD is an extension to the studies of the $D^1\Pi_u$ state in H_2 and D_2 (Dickenson *et al* 2010, 2011). The measurements were obtained with the vacuum ultraviolet (VUV) Fourier transform spectrometer (FTS) at the DESIRS beamline of the synchrotron SOLEIL. The line widths of transitions probing Π^+ levels for all three hydrogen isotopomers are used to verify scaling laws for the predissociation in the $D^1\Pi_u$ state.

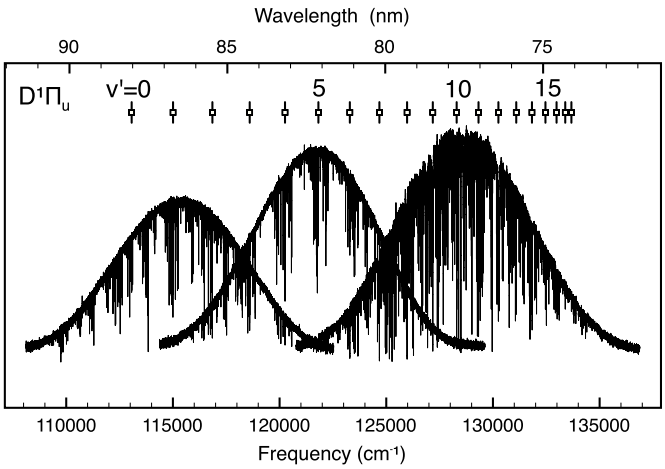

Figure 1. An overview of the recorded spectra analysed in this study. The band heads of the $D^1\Pi_u$ state are indicated up to $v' = 18$. Other prominent spectral features are associated with the $B^1\Sigma_u^+$, $B'^1\Sigma_u^+$ and $C^1\Pi_u$ states below the $n = 2$ dissociation limit (Ivanov *et al* 2010) and $B''^1\Sigma_u^+$ states above $n = 2$. Above the ionization limit, 124 568 cm^{-1}(Sprecher *et al* 2010) many auto-ionization resonances appear in the spectrum.

2. Experiment

The VUV FTS is a scanning wavefront division interferometer operational from 40 to 200 nm. It has been used previously in a study of the Lyman and Werner bands of HD (Ivanov *et al* 2010). We provide only a short description of the experimental configuration; for a detailed explanation we refer to the works of de Oliveira *et al* (2009, 2011). The light source is undulator based and can be tuned continuously to produce a bell-shaped output window spanning approximately 5 nm as illustrated in figure 1. The undulator radiation passes through a windowless T-shaped cell, 10 cm in length, which contains a quasi-static HD sample, slowly flowing out either side of the cell. The purity of the HD gas is estimated at $\geqslant$99% with some traces of H_2 resulting in weak spectral features associated with H_2 Lyman bands in the low-energy region. The HD is cooled to a temperature of 100 K by liquid nitrogen which flows over the outside of the T-shaped cell.

Each measurement was recorded by taking 512 kilo samples of data over the optical path difference, resulting in an instrumental width of 0.33 cm^{-1}. The final spectral windows were averaged over 100 individual interferograms and took about 2 h to accumulate. The pressure inside the absorption cell can be regulated resulting in a change in the column density. Spectra were recorded at sufficient column density so that transitions appear with optimal signal-to-noise ratio but not saturated. A spectral range spanning from 112 000–134 000 cm^{-1} (75–90 nm) was covered by three spectral windows each set at a different central wavelength as shown in figure 1.

The wavelength scale in the FT spectra display a strict linearity so that only one fixed point is required for a calibration. This is provided by a transition in atomic argon present in the gas filter which is used to remove higher order harmonics of the selected wavelength produced by the undulator. The transition is the $(3p)^5(^2P_{3/2})9d([3/2])-(3p)^6$ $^1S_0$ at 125 718.13 cm^{-1} known to an accuracy of 0.03 cm^{-1} (Sommavilla *et al* 2002).

3. Theory

The predissociation of the $D^1\Pi_u$ state is due to a strong Coriolis coupling to the continuum of the $B'^1\Sigma_u^+$ state (Monfils 1961). Due to the Σ^+ character of the continuum, transitions probing levels of Π^- symmetry are not affected by this interaction and are only very weakly predissociated due to coupling with the lower lying $C^1\Pi_u$ continuum (Glass-Maujean *et al* 2010). A single continuum interacting with a bound state is described by Fano's theory (Fano 1961) and produces broadened asymmetric absorption profiles described by the Fano function. For more details we refer to our previous works (Dickenson *et al* 2010, 2011). The widths, broadened by lifetime shortening due to the predissociation are given by

$$\Gamma_{v'} = 2\pi\,|\langle\psi_{B'\epsilon}|H(R)|\psi_{Dv'}\rangle|^2, \tag{1}$$

where $\psi_{B'\epsilon}$ and ψ_D are the wavefunctions of the B' continuum and the discrete D state, respectively. Here, the energy value B'_ϵ of the B' state is taken equal to the non-perturbed energy of the discrete level $D_{v'}$. The rotational operator, $H(R)$, is the $\vec{L}\cdot\vec{R}$ operator (also responsible for the Λ-doublet splitting) which causes the predissociation widths of levels $D_{v'}$ to scale as

$$\Gamma_{v'} \propto \frac{1}{\mu^2}J(J+1), \tag{2}$$

where μ is the reduced mass of the molecule and J is the rotational quantum number. The reduced mass for the three isotopomers H_2, HD and D_2 are 0.5, 0.67 and 1.0 amu, respectively.

4. Results and discussion

The region above the second dissociation limit in HD is a complex multi-line spectrum that when cooled to liquid nitrogen temperatures consists of six overlapping Rydberg series (Dehmer and Chupka 1983). The absorption spectrum is heavily congested making a complete analysis of all spectral features a challenge. In particular, the $D^1\Pi_u$ state is recognizable from the broadened Beutler–Fano profiles, aiding the assignment thereof. Our assignments agree with the previous works of Monfils (1965) and Dehmer and Chupka (1983) which are accurate to within 4–5 cm^{-1}. The largest discrepancy occurs for the $D^1\Pi_u(v' = 9)$–$X^1\Sigma_g^+(v'' = 0)$ band, differing from the present line positions by $\sim$ 8 cm^{-1} possibly attributable to wavelength drive slippage of the monochromator, as mentioned by the authors. Beyond $v' = 16$ the identifications are aided by the calculations of the band heads made by Kołos and Rychlewski (1976) accurate to within 1–3 cm^{-1}. From an estimate of the Λ-doublet splitting, the $Q(1)$ transitions could be identified. The $R(1)$ transitions beyond $v' = 15$ were too weak to be observed.

The Q-branch transitions, observed as narrow resonances limited by Doppler broadening, were observed up to $v' = 18$

Table 1. Transition frequencies of Q-branch transitions probing levels of Π^- symmetry. Δ represents a comparison with the previous measurements of Monfils (1965) for $v' = 0$–6 and Dehmer and Chupka (1983) for $v' = 7$–16, defined as the present measurement minus the previous measurements. All values in cm^{-1}.

Transition frequency		Δ	Transition frequency		Δ
	D–$X(0,0)$			D–$X(1,0)$	
$Q(1)^a$	112 975.18	1.11	$Q(1)^a$	114 916.47	5.10
$Q(2)$	112 886.03	1.35	$Q(2)$	114 822.09	−0.07
$Q(3)$	112 753.22	1.77	$Q(3)$	114 684.45	2.26
	D–$X(2,0)$			D–$X(3,0)$	
$Q(1)^a$	116 760.16	2.73	$Q(1)^a$	118 508.76	2.42
$Q(2)^a$	116 663.06	1.69	$Q(2)^a$	118 407.81	2.58
$Q(3)$	116 518.29	1.36	$Q(3)$	118 256.35	1.39
	D–$X(4,0)$			D–$X(5,0)$	
$Q(1)^a$	120 164.47	−1.01	$Q(1)$	121 729.21	0.90
$Q(2)$	120 059.79	0.96	$Q(2)$	121 620.99	0.99
$Q(3)$	119 900.37	0.46	$Q(3)$	121 459.67	1.20
	D–$X(6,0)$			D–$X(7,0)$	
$Q(1)$	123 203.12	1.95	$Q(1)$	124 588.35	1.25
$Q(2)$	123 091.11	1.09	$Q(2)$	124 472.72	
$Q(3)$	122 924.14	0.69	$Q(3)$	124 300.33	
	D–$X(8,0)$			D–$X(9,0)$	
$Q(1)$	125 885.02	1.62	$Q(1)$	127 091.67	−7.23
$Q(2)$	125 765.66		$Q(2)$	126 968.71	
	D–$X(10,0)$			D–$X(11,0)$	
$Q(1)$	128 208.79	5.29	$Q(1)$	129 234.35	1.15
$Q(2)$	128 082.25		$Q(2)$	129 103.84	
	D–$X(12,0)$			D–$X(13,0)$	
$Q(1)$	130 166.57	−0.43	$Q(1)$	131 002.36	2.56
$Q(2)$	130 032.21		$Q(2)$	130 864.00	
	D–$X(14,0)$			D–$X(15,0)$	
$Q(1)^b$	131 737.82	−1.88	$Q(1)$	132 369.36	3.66
$Q(2)$	131 595.19				
	D–$X(16,0)$			D–$X(17,0)$	
$Q(1)^b$	132 891.54	−0.06	$Q(1)$	133 299.89	
	D–$X(18,0)$				
$Q(1)$	133 588.59				

[a] Saturated.
[b] Blended.

Table 2. Transition frequencies of R-branch transitions probing levels of Π^+ symmetry. Δ represents a comparison with the previous measurements of Monfils (1965) for $v' = 0$–6 and Dehmer and Chupka (1983) for $v' = 7$–16 defined as the present measurement minus the previous measurements. Γ represents the predissociation width. All values in cm^{-1}.

Transition frequency	Γ	Δ	Transition frequency	Γ	Δ
D–$X(0,0)$			D–$X(1,0)$		
$R(0)^a$ 113 066.07		−0.75	$R(0)^a$ 115 005.76		1.17
$R(1)^a$ 113 068.72		2.84	$R(1)^a$ 115 000.70		−4.21
D–$X(2,0)$			D–$X(3,0)$		
$R(0)^a$ 116 851.42		4.44	$R(0)^a$ 118 598.93		0.79
$R(1)^a$ 116 846.89		1.53	$R(1)^a$ 118 591.70		2.86
D–$X(4,0)$			D–$X(5,0)$		
$R(0)$ 120 254.63	2.4	0.08	$R(0)$ 121 819.48	2.6	0.78
$R(1)$ 120 240.26	7.3	−1.05	$R(1)$ 121 801.44	6.0	2.62
D–$X(6,0)$			D–$X(7,0)$		
$R(0)$ 123 293.27	2.8	0.43	$R(0)$ 124 678.40	2.4	0.70
$R(1)$ 123 271.74	6.8	0.91	$R(1)$ 124 652.34	5.8	0.56
D–$X(8,0)$			D–$X(9,0)$		
$R(0)$ 125 974.74	2.3	1.15	$R(0)$ 127 181.58	2.2	−7.82
$R(1)$ 125 945.60	6.8	0.09	$R(1)$ 127 148.23	6.4	−8.97
D–$X(10,0)$			D–$X(11,0)$		
$R(0)$ 128 298.77	2.5	3.67	$R(0)$ 129 324.08	2.1	2.28
$R(1)$ 128 261.88	6.2	3.18	$R(1)$ 129 282.73	5.9	1.23
D–$X(12,0)$			D–$X(13,0)$		
$R(0)^b$ 130 256.22	2.1	−3.38	$R(0)$ 131 092.40	1.2	1.60
$R(1)$ 130 211.60	4.8	−1.70	$RR(1)^b$ 131 043.31	3.5	2.31
D–$X(14,0)$			D–$X(15,0)$		
$R(0)$ 131 827.56	1.3	−1.54	$R(0)^b$ 132 459.67	0.9	3.37
$R(1)$ 131 773.73	5.4	−2.57	$R(1)$ 132 400.58	5.5	
D–$X(16,0)$			D–$X(17,0)$		
$R(0)$ 132 980.87	1.7	−1.53	$R(0)$ 133 389.31	1.1	
D–$X(18,0)$					
$R(0)^b$ 133 677.72					

[a] Saturated.
[b] Blended.

and are listed in table 1. The R-branch transitions which are broadened for $v' \geqslant 4$, were also observed up to $v' = 18$ ($R(0)$ transitions only). Transition energies and predissociated widths for these transitions are listed in table 2. All line positions and predissociated widths listed in the tables stem from a deconvolution procedure as described in the previous work on D_2 (Dickenson *et al* 2011). Briefly, the absorption profiles are first convoluted with a Gaussian function representative of the Doppler profile at 100 K. In the second step, the Beer–Lambert law is included, accounting for the nonlinear absorption depth. Finally, the resulting profiles are convoluted with the instrument function and the fit parameters are then optimized by a standard least-squares fitting routine. Included in the parameters are the points to an unbounded, cubic spline fit of the background. These are optimized along with the line shape parameters resulting in a fit of the background. A sample fit of the $Q(1)$, $R(1)$ and $R(0)$ transitions belonging to the D–X (6,0) band is shown in figure 2. The $Q(1)$ transition has a width of approximately 0.6 cm^{-1} which stems from the contribution of the instrument width of 0.33 cm^{-1} and the Doppler width of 0.5 cm^{-1} and represents the limiting resolution for the particular configuration of the FTS used.

In this analysis of the line widths, the Beutler–Fano asymmetry of the line shape, represented by the Fano q-parameter was included by fixing the q-values to their theoretical prediction. Upon mass-scaling the q-parameters ($q \propto \mu$), it follows that $q \sim -25$ for $R(0)$ and $q \sim -15$ for $R(1)$ transitions in HD (Glass-Maujean 1979, Dickenson *et al* 2011). The present data did not permit to perform a reliable two-parameter fit to extract both q and Γ. This is in part due to the method of recording the spectra in absorption against a fluctuating continuum level. For further discussion, see the previous work on D_2 (Dickenson *et al* 2011).

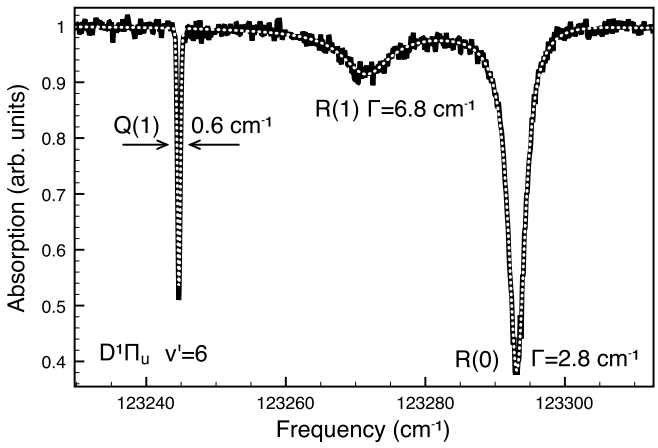

Figure 2. Detailed spectrum of the $D^1\Pi_u(v' = 6)$–$X^1\Sigma_g^+(v'' = 0)$ band with $R(0)$, $R(1)$ and $Q(1)$ transitions. The dotted white line represents a least-squares fit of the data with the appropriate convoluted functions (see the text for details).

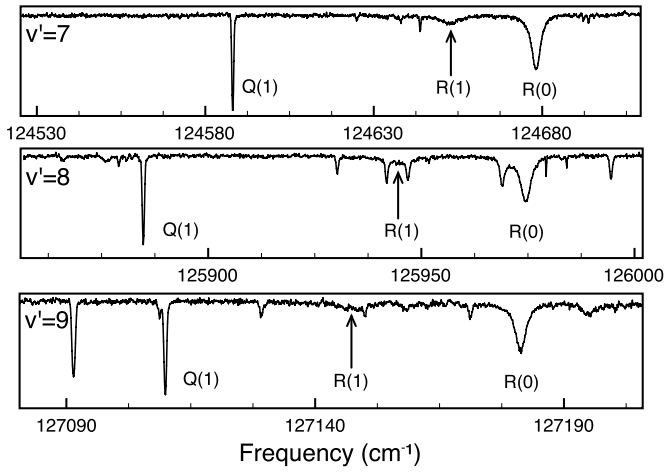

Figure 3. Small portions of spectral windows containing the $D^1\Pi_u(v' = 7$–$9)$–$X^1\Sigma_g^+(v'' = 0)$ bands of HD. These bands are predissociated and display typical broadened Beutler–Fano profiles.

4.1. Spectroscopic results

The Q-branch transitions, i.e. transitions probing states of Π^- symmetry and transitions belonging to bands with $v' \leqslant 3$ are not predissociated and observed as narrow features with width, ∼0.6 cm^{-1}, equal to the Doppler width of HD at 100 K convoluted with the instrument width. Uncertainty in the reported line positions in table 1 and for the unpredissociated bands listed in table 2 is estimated at 0.06 cm^{-1}. For slightly saturated lines, blended lines and weak lines the uncertainty estimate increases to 0.08 cm^{-1}.

The R- and P-branch transitions are observed as broadened due to the life-time shortening caused by predissociation. Several small portions of the spectra are displayed in figure 3 including the $D^1\Pi_u(v' = 7$–$9)$–$X^1\Sigma_g^+$ bands which display typical predissociation broadening. These transitions were fitted with convoluted profiles and the resultant line positions and widths are listed in table 2. The $P(2)$ and $R(2)$ transitions for bands with $v' \geqslant 3$ were observed as extremely weak as a result of the fact that most of the rotational population

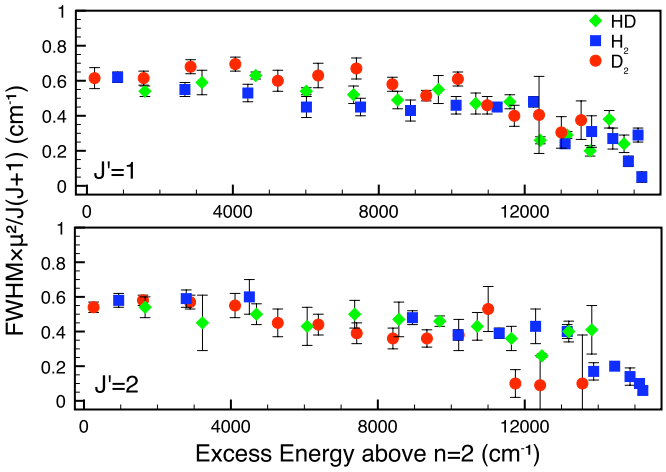

Figure 4. The predissociation widths scaled by multiplying by the reduced mass squared (μ^2). The energy scale on the x-axis is referenced to the $n = 2$ dissociation limit of each molecule as determined by Eyler and Melikechi (1993). See the text for details.

resides in the $J'' = 0$ and 1 levels. We estimate an uncertainty of 0.20 cm^{-1} on the line positions of the $R(0)$ transitions which were observed to be ∼3 cm^{-1} broad and a 0.4 cm^{-1} uncertainty estimate on the $R(1)$ transitions observed at widths of ∼7 cm^{-1}. There were a number of blended lines, most of which could still be fitted. Those lines affected severely by blending are indicated in the table and the estimated line position uncertainty is doubled.

4.2. Predissociated widths

Figure 4 depicts the predissociated widths as a function of the excess energy above the $n = 2$ dissociation limit for all three stable isotopomers, H_2 and D_2 as determined in previous work (Dickenson *et al* 2010, 2011) and the newly determined HD widths. The dissociation limits used for H_2, D_2 and HD were H($1S$)+H($2S$), D($1S$)+D($2S$) and H($1S$)+D($2S$), respectively (Eyler and Melikechi 1993). The measured widths have been scaled by their respective reduced masses squared and the rotational dependence has been removed by dividing through by $J(J + 1)$. The data for H_2 between 5000 and 8000 cm^{-1} are missing due to blending with the B'' state in this region. Agreement between the three isotopomers for both $J' = 1$ (derived from $R(0)$ transitions) and $J' = 2$ (derived from $R(1)$ transitions) rotational levels is good yielding further proof of the applicability of the simple two-state model to the predissociation of the $D^1\Pi_u$ state in all three stable hydrogen isotopomers. At the present level of accuracy, the data indicate that u–g symmetry breaking effects in HD do not play a role in the predissociated life-times and that the predissociation can be fully described by the $|\langle\psi_{B'\epsilon}|H(R)|\psi_{Dv'}\rangle|$ interaction.

4.3. Λ-doublet

The Λ-doublet splitting, as depicted in figure 5, was determined by adding the ground state level energy to the Q-branch transitions (Komasa *et al* 2011) and subtracting this from the R-branch transitions probing the same J' but opposite

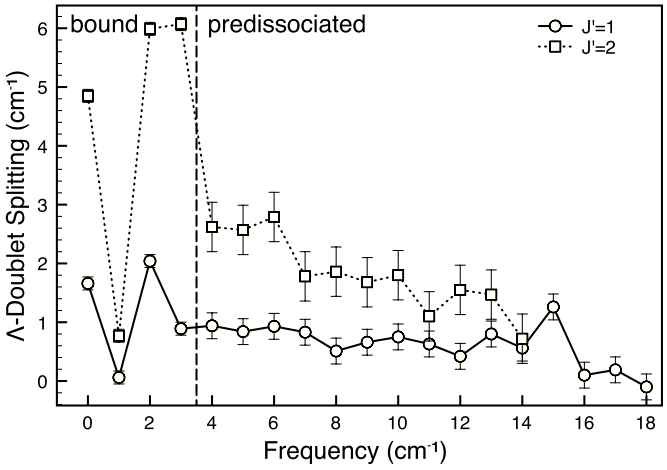

Figure 5. The Λ-doublet splittings in the $D^1\Pi_u$ state of HD for the $J' = 1$ and 2 rotational states. The lines joining the points are to guide the eye.

(e)–(f) parity. The results mirror those obtained for H_2 and D_2. The Λ-doublet splittings follow an erratic behaviour for $v' < 4$ caused by the interactions between the discrete B' and D state levels. For $v' \geqslant 4$, it follows a relatively smoothly decaying trend similar as in the observations on H_2 and D_2 (Dickenson *et al* 2010, 2011). If the assumption can be made that the B' state is the sole perturber causing the Λ-doubling, the Λ-doublet splitting can be represented as

$$\Lambda_{v'}(J') \propto \sum_{B'v,\epsilon} \frac{|\langle\psi_{B'v,\epsilon}|H(R)|\psi_{Dv'}\rangle|^2}{E_{\Pi_v^+} - E_{B'v,\epsilon}}, \qquad (3)$$

where summation over all B' levels includes the bound levels below $n = 2$ and an integral over the B' continuum. Interaction with the B' levels of $^1\Sigma^+$ symmetry causes the $\Pi^+(e)$ levels of the $D^1\Pi_u$ state to shift upwards, while the $\Pi^-(f)$ levels are unaffected. Similarly as in the deviation of the predissociation widths, the Λ-doublet splitting then scales like $\mu^{-2}J(J+1)$. The present results on HD and the results of H_2 (Dickenson *et al* 2010) perfectly match this scaling, while the Λ-doublet splittings in D_2 (Dickenson *et al* 2011) are somewhat too large in this comparison.

5. Conclusion

The VUV FTS observations on the $D^1\Pi_u$ state have been extended to HD. This work represents the highest resolution study on this state performed so far. The predissociated line shapes were analysed resulting in predissociated line widths determined to a high level of accuracy. The present and previous studies show, through the mass scaling and rotational scaling, that the predissociation in the Π^+ parity states of the $D^1\Pi_u$ state can be modelled by a rotational interaction with the continuum of the $B'^1\Sigma_u^+$ state. In the case of HD, the u–g symmetry breaking does not play a role in the predissociated widths at the present level of accuracy.

Acknowledgments

The authors are grateful to the SOLEIL staff scientists L Nahon, N de Oliveira and D Joyeux for the hospitality and for the collaboration. Dr A Heays is thanked for valuable advice regarding the fit model. The EU provided financial support through the transnational funding scheme. This work was supported by the Netherlands Foundation for Fundamental Research of Matter (FOM). The authors thank two anonymous referees for valuable suggestions.

References

Abgrall H and Roueff E 2006 *Astron. Astrophys.* **445** 361
de Oliveira N, Joyeux D, Phalippou D, Rodier J C, Polack F, Vervloet M and Nahon L 2009 *Rev. Sci. Instrum.* **80** 043101
de Oliveira N, Roudjane M, Joyeux D, Phalippou D, Rodier J C and Nahon L 2011 *Nature Photon.* **5** 149
Dehmer P and Chupka W 1980 *Chem. Phys. Lett.* **70** 127
Dehmer P and Chupka W 1983 *J. Chem. Phys.* **79** 1569
Dickenson G D *et al* 2010 *J. Chem. Phys.* **133** 144317
Dickenson G D *et al* 2011 *Mol. Phys.* **109** 2693
Eyler E E and Melikechi N 1993 *Phys. Rev.* A **48** R18
Fano U 1961 *Phys. Rev.* **124** 1866
Glass-Maujean M 1979 *Chem. Phys. Lett.* **68** 320–3
Glass-Maujean M, Jungen C, Schmoranzer H, Knie A, Haar I, Hentges R, Kielich W, Jänkälä K and Ehresmann A 2010 *Phys. Rev. Lett.* **104** 183002
Ivanov T, Dickenson G, Roudjane M, de Oliveira N, Joyeux D, Nahon L, Tchang-Brillet W-Ü L and Ubachs W 2010 *Mol. Phys.* **108** 771
Kołos W and Rychlewski J 1976 *J. Mol. Spectrosc.* **62** 109
Komasa J, Piszczatowski K, Łach G, Przybytek M, Jeziorski B and Pachucki K 2011 *J. Chem. Theory Comput.* **7** 3105
Monfils A 1961 *Acad. Roy. Belg. Bull. Cl. Sci.* **5** 599
Monfils A 1965 *J. Mol. Spectrosc.* **15** 265
Sommavilla M, Hollenstein U, Greetham G and Merkt F 2002 *J. Phys. B: At. Mol. Opt. Phys.* **35** 3901
Sprecher D, Liu J, Jungen C, Ubachs W and Merkt F 2010 *J. Chem. Phys.* **133** 111102
Takezawa S and Tanaka Y 1972 *J. Chem. Phys.* **56** 6125